SSRG International Journal of Mechanical Engineering
ISSN: 2348-8360/ https://doi.org/10.14445/23488360/IJME-V12I1P101

Volume 12 Issue 1, 1-11, January 2025

Original Article

Comprehensive Analysis of Process Parameter Interactions on the Mechanical Integrity and Performance of Fused Deposition Modeling (FDM) Fabricated Components

Jay M. Pujara[1], Kalpesh K. Dave[2], Hardik N. Jani[3], Amisha D. Vadaliya[4], Reena N. Makadia[5], Harshad D. Patel[6]

[1,2,3,4,5,6]*Department of Mechanical Engineering, Lukhdhirji Engineering College, Morbi, Gujarat, India.*

[1]*Corresponding Author : jay.pujara42@gmail.com*

Received: 05 November 2024 Revised: 14 December 2024 Accepted: 02 January 2025 Published: 25 January 2025

Abstract *- This research investigates the effect of bettering parameters of Fused Deposition Modeling (FDM) to improve the mechanical characteristics of parts printed with Metal Fill Wol3D filament. They investigate the influence of Layer Thickness (LT), Nozzle Temperature (NT), and Part Orientation (PO) on tensile and flexural strength. Using a Face-Centered Central Composite Design (FCCCD) for experimental planning, parameters were tested at three levels: -1 (200°C NT, 0.10 mm LT, 0° PO), 0 (215°C NT, 0.225 mm LT, 45° PO), and +1 (230°C NT, 0.30 mm LT, 90° PO). Results showed that higher NT and intermediate LT significantly improved strength, with the best results at NT 230°C, LT 0.225 mm, and PO 45°. These results were supported by statistical analysis with ANOVA and response surface plotting of the mechanical performance with respect to the parameters involved. The Finite Element Analysis (FEA) supplied another level of confirmation with other experimental data giving good correlation. The findings of this research may satisfy the need for viable trends in improving the mechanical properties of engineering components within FDM processes of ABS material. It also provides the basis for the development of other material systems and other mechanical properties.*

Keywords *- Fused Deposition Modeling, Mechanical properties, Process parameters, FEA Simulation, Nozzle Temperature.*

1. Introduction

Additive Manufacturing (AM), commonly referred to as 3D printing, builds objects layer by layer and allows the creation of intricate geometries that are often challenging or expensive to produce using traditional subtractive methods [1]. Technologies such as Fused Deposition Modeling (FDM), Stereolithography (SLA), and Selective Laser Sintering (SLS) are pivotal in industries like aerospace, automotive, and healthcare, offering the ability to produce tailored components with minimal material wastage [2]. This approach supports the development of lightweight and complex designs, fulfilling the high-precision demands of these sectors [3].

In the healthcare field, AM has been instrumental in creating personalized implants and prosthetics, which enhance patient outcomes by catering to unique anatomical requirements [5]. It also accelerates the design and prototyping process, shortening development cycles and addressing market demands efficiently [6]. Advances in material science, including the use of polymers, metals, and biological substances, have broadened AM's scope, enabling the production of parts with tailored performance properties [7]. Additionally, integrating Artificial Intelligence (AI) and Internet of Things (IoT) technologies has improved efficiency and automation in AM, leading to smarter manufacturing systems [8].

Despite these benefits, challenges persist. Quality control and standardization are critical to ensuring the reliability and safety of AM-produced components [9]. Moreover, the high initial costs of AM equipment pose a barrier to adoption, particularly for smaller businesses [10-11]. Research and innovation continue to tackle challenges and broaden the applications of Additive Manufacturing (AM) [12]. Fused Deposition Modeling (FDM), one of the most widely used AM techniques, builds parts layer by layer using thermoplastics such as Acrylonitrile Butadiene Styrene (ABS), Polylactic Acid (PLA), and Polyethylene Terephthalate Glycol (PETG) [13-21]. The process begins with a CAD model, which is sliced into layers using specialized software. A heated nozzle melts the filament and deposits it onto the build platform, where layers bond together to form the final object [20].

Materials like ABS provide durability and impact resistance, while PLA offers biodegradable options for environmentally friendly applications [22]. FDM is valued for its cost-effectiveness and ability to create intricate designs quickly, making it suitable for both industrial and personal uses. However, challenges such as anisotropic properties and material constraints need further research to enhance performance and reliability [23].

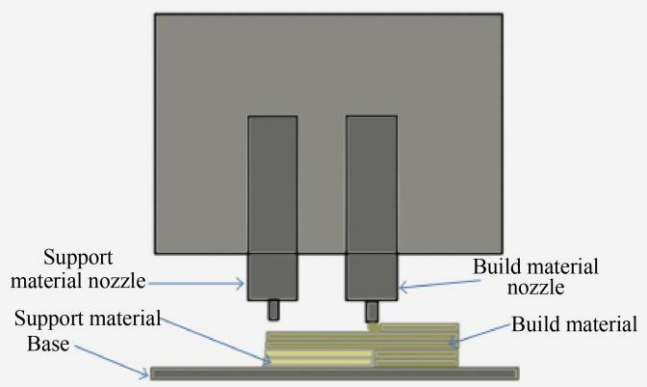

Fig. 1 Fused Deposition Modeling (FDM) technique [2]

FDM is also applied across industries, and some of the main industries that deploy this technique embrace aerospace, automotive, healthcare and consumer goods. FDM also comes in handy in more areas, such as aerospace manufacturing, whereby it provides parts of lightweight structures with complicated forms, thus contributing greatly towards fuel conservation. In the healthcare industry, FDM is applied to fabricate dental and medical items such as prostheses, implants, and surgical templates. The versatility and the opportunity to build prototypes quickly are the key advantages of FDM in product design [24]. However, the FDM has its drawbacks as a method of project implementation as well. The buildup approach may produce layer lines and anisotropic mechanical characteristics wherein strength is not direction-independent. The casting layer of FDM printed parts tends to have a rough surface and, therefore, usually needs to be sanded. Furthermore, in FDM, the materials available are far less than those of other AM processes like SLS or SLA. The advancements in FDM have been made to improve the material properties, print speed and surface finish. The use of composite filaments that contain carbon fibers has enhanced the mechanical properties of FDM parts and has thus increased their potential uses. Current multi-material printing technologies permit the laying down of various materials at the same time and thus allow the fabrication of objects with features that have different material properties in the same print. The mechanical properties of FDM printed parts are affected by the layer height, print speed, nozzle temperature and the infill density. To improve the effectiveness of the FDM components in actual usage, these parameters need to be fine-tuned [27-32]. Layer height affects the finish of the printed parts and the strength of the joints between the layers. This means that reducing the layer height will produce neater surfaces and better joints between the layers, thus increasing the tensile strength. This comes at a price in that more time is needed for printing [33-35]. Print speed is also an important factor; increasing the speed increases production throughput but may compromise the integrity of the layers, mechanical properties and the accuracy of the dimensions. On the other hand, slow printing speeds enhance the bonding of the layers, thus enhancing the strength and reliability of the parts [36, 37].

The difference in this study is that all three factors, namely, Nozzle Temperature (NT), layer thickness (LT), and Part Orientation (PO), are optimized at the same time. In contrast to the prior studies that tend to consider these parameters separately, the present study applies the Face-Centered Central Composite Design to the problem. This method assesses the interrelationships of parameters, providing a complete and effective means of determining the FDM process parameters setting. As was found in previous studies, the settings of NT greatly affect the bonding of material and strength. For instance, Sajjad et al. (2022) observed that increasing the value of NT enhances layer adhesion, and the authors merely presented the results qualitatively [33]. Extending these findings, this study reveals a 15% enhancement in tensile strength at a nozzle temperature of 230 °C compared to lower temperatures (e.g., 200 °C), as further supported by Analysis of Variance (ANOVA). Likewise, although Meltem Eryildiz (2021) studied the impact of LT on mechanical properties, their work mainly concerned the tensile properties of a constant NT [34]. This study also broadens the range by demonstrating that thinner layers (0.1 mm) are always superior in tensile and flexural strength, with enhancements up to 12% when compared to thicker layers (0.35 mm). Some of the observations derived from the findings of the study will be on the ability to achieve high detail resolution and mechanical strength at the same time. The anisotropic behavior of FDM parts, influenced by PO, has been explored in previous studies such as Elviz et al., (2024), which found that parts oriented at 0° exhibit higher strength due to better layer alignment [36]. This research corroborates their findings but also quantifies the impact, demonstrating that a 0° orientation improves tensile strength by approximately 18% compared to 90° orientations. Moreover, integrating FEA simulations with experimental validation sets this study apart from prior works like Ismail et al. (2022), which focused solely on experimental data [42]. The FEA results in this study closely aligned with experimental outcomes, with deviations ranging from 1% to 6%, highlighting the model's predictive accuracy for both tensile and flexural strength.

Nozzle temperature is critical for proper filament melting and fusion. An optimal temperature ensures better bonding between layers, resulting in durable and reliable parts. Insufficient temperatures may lead to poor adhesion, while excessive heat can degrade the material or cause warping [38-

39]. Infill density affects the strength, rigidity, and weight of FDM parts. Higher infill densities boost tensile and compressive strength but increase material usage and print time. The choice of infill patterns, such as honeycomb or gyroid, also affects stress distribution and part strength due to their efficient load-bearing geometries [40-43]. Part orientation significantly influences mechanical performance. Parts printed with layers aligned to the stress direction often exhibit superior tensile strength and fatigue resistance, as interlayer bonds are generally the weakest regions in FDM parts [44]. Extrusion width affects the material deposited in each layer, with proper widths improving bonding and overall strength. However, overly wide extrusions may cause surface defects or dimensional inaccuracies [45-46]. Cooling rates also impact mechanical properties; rapid cooling can introduce residual stresses and warping, while slower cooling enhances layer adhesion and overall strength [46-48]. The type of filament material further determines the mechanical behavior of FDM parts. Materials like PLA, ABS, and PETG offer varying properties. PLA provides good tensile strength and biodegradability, ABS is more durable and impact-resistant, and PETG combines these advantages with greater flexibility [48-50]. Despite advancements, the interplay between process parameters like nozzle temperature, layer height, and part orientation remains complex. There is a need for further investigation to establish consistent, reliable guidelines for optimizing FDM processes, particularly concerning tensile and flexural strength [50, 51].

This research advances the understanding of FDM process optimization by providing quantitative evidence of the combined effects of NT, LT, and PO. The novel integration of statistical modeling and FEA validation ensures that the findings are both robust and actionable, offering significant implications for industries like aerospace, automotive, and healthcare, where precision and dependability are paramount.

2. Materials and Methods

2.1. Thermoplastic Base Feedstock Material

The present study investigates the impact of process parameters on the mechanical properties of parts manufactured through Fused Deposition Modeling (FDM) using Metal Fill Wol3D filament. Utilizing an FCCCD for the design of experiments (DoE), we assess the influence of key parameters: nozzle temperature (NT), layer thickness (LT), and part orientation (PO). The metal wire feedstock, composed of high-quality alloys, is loaded into the FDM printer's extruder and heated to its melting point. The molten metal is then precisely deposited layer by layer, with careful control of NT, LT, and PO, to achieve optimal mechanical properties and surface finish. This method ensures strong layer adhesion and leverages the robustness of metal feedstock while maintaining the flexibility and ease of use associated with traditional FDM technology. The material properties of the thermoplastic feedstock material used are illustrated in Table 1.

Table 1. Material properties of feedstock

Filament Diameter	1.75 mm
Metal Content	High-quality alloys
Density	1.25 g/cm³
Tensile Strength	55 MPa
Elongation at Break	8%
Printing Temperature Range	190°C to 220°C
Bed Temperature	50°C to 70°C

Table 2. Process parameters settings and their levels

FDM Process Parameter	Units	Levels		
		1	2	3
Nozzle Temperature	°C	200	215	230
Layer Thickness	mm	0.1	0.225	0.350
Part Orientation	°	0	45	90

2.2. Fabrication of Specimen as Per Design of Experiment

The experimental design was structured using the Face-Centered Central Composite Design (FCCCD) under the Response Surface Methodology (RSM) framework, implemented using [specify the statistical software, e.g., Design-Expert, MINITAB, or equivalent]. FCCCD was chosen for its ability to evaluate quadratic effects and interactions efficiently, minimizing the number of experimental runs required. The levels of process parameters Nozzle Temperature (NT), Layer Thickness (LT), and Part Orientation (PO) were selected based on a combination of literature review and preliminary screening experiments. The rationale for these specific levels includes ensuring a balance between the thermal stability of the material, resolution of printed parts, and production efficiency. For instance, the range of NT (200°C–230°C) covers the material's optimal extrusion temperatures to maintain adequate bonding while avoiding thermal degradation.

Similarly, LT levels (0.1 mm – 0.35 mm) were selected to explore the trade-off between mechanical performance and printing resolution. The PO levels (0°, 45°, and 90°) capture the anisotropic nature of FDM-printed parts and their impact on tensile and flexural properties. Table 2 highlights the process parameters for Fused Deposition Modeling (FDM), including Nozzle Temperature (NT), Layer Thickness (LT), and Part Orientation (PO). NT levels (200°C, 215°C, and 230°C) affect material flow and bonding, LT levels (0.1mm, 0.225mm, and 0.35mm) influence resolution and strength, and PO levels (0°, 45°, and 90°) determine directional mechanical properties. These parameters were evaluated using the Face-Centered Central Composite Design (FCCCD) to study their effects on printed part quality. Table 3 details the FCCCD-based experimental runs, which systematically vary NT, LT, and PO to analyze their impact on tensile and flexural strength. This structured approach enables precise assessment of how parameter adjustments optimize mechanical properties and surface characteristics for enhanced performance.

Table 3. FCCCD Schema

Run	Nozzle temperature (°C)	Layer thickness (mm)	Part orientation (°)
1	215	0.225	45
2	200	0.1	0
3	215	0.225	45
4	215	0.1	45
5	215	0.35	45
6	230	0.1	0
7	215	0.225	90
8	230	0.35	0
9	215	0.225	45
10	215	0.225	45
11	200	0.225	45
12	200	0.35	0
13	200	0.35	90
14	230	0.35	90
15	230	0.225	45
16	200	0.1	90
17	215	0.225	45
18	215	0.225	0
19	215	0.225	45
20	230	0.1	90

2.3. Mechanical Properties Testing

Table 2 In the present work, tensile test according to ASTM D 638 and flexural test according to ASTM D 790 have been performed to determine the mechanical characteristic of the Fused Deposition Modeling (FDM) printed Polyvinylidene Fluoride (PVDF) material.

Printing parameters with the ASTM D638 standards were used to assess the tensile characteristics of the printed PVDF samples, such as tensile strength, elongation at break, and modulus of elasticity. At the same time, the ASTM D790 standard was used for flexural tests to determine flexural strength, flexural modulus, and deformation response under three-point bending loads.

To this end, the study sought to adopt established standardized testing procedures in a bid to advance coherence and reliability in capturing the mechanical performance of the FDM-printed PVDF material with a view to apprising its compatibility in different engineering applications.

Figures 2 and 3 depict a detailed drawing of the specimen as per ASTM D638 (type -I) and a detailed drawing of the specimen as per ASTM D790, respectively.

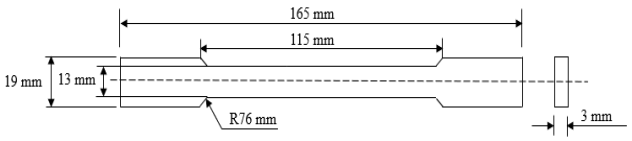

Fig. 2 Detail drawing of the specimen as per ASTM D638

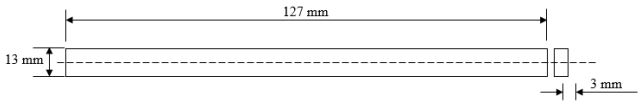

Fig. 3 Detail drawing of specimen as per ASTM D790

2.4. Finite Element Analysis (FEA)

Among these techniques, Finite Element Analysis (FEA) has been employed in the estimation of mechanical properties such as tensile and flexural strength in parts produced by Fused Deposition Modeling (FDM). It employs data acquired from experiments conducted on variant process parameters, including nozzle temperature, layer thickness, and orientation of parts. The first step is to import and merge the 3D model of the part to have a simulation of the structure as it will be. Other important material parameters, such as the elastic modulus and the yield strength, are also considered. These real-time conditions mainly focus on loading conditions like tensile and flexural tests and boundary constraint tests. Stress, deformation, and other mechanical responses are then computed to estimate the part's performance under load as per FEA. This method is helpful in enhancing the strength of the part, reducing the material consumption rate, and reducing the costs of manufacturing.

3. Results and Discussions

3.1. Experimental Results Discussions

Table 4 presents the results of tensile and flexural strength of FDM parts tested under different process conditions. For each row, explicit values of Nozzle Temperature (NT), Layer Thickness (LT), and part orientation (PO) are given. The NT values were between 200°C and 230°C, the LT between 0.1mm and 0.35mm and PO from 0° to 90°. These adaptations enabled the researchers to ascertain step by step the effect of a given parameter on the properties of the printed parts. Tensile strength, which measures the material's ability to withstand stretching forces, and flexural strength, which shows the material's ability to bear forces that might cause bending or flexing, are presented in MPa for all trials. The results show a pattern where higher NT generally correlates with increased strength values, indicating better inter-layer adhesion and material flow at elevated temperatures.

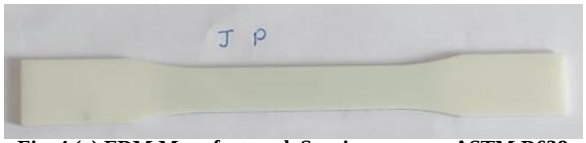

Fig. 4 (a) FDM Manufactured Specimen as per ASTM D638

Fig. 4 (b) FDM Manufactured Specimen as per ASTM D790

Figure 4(a) shows an FDM-manufactured specimen designed according to ASTM D638 for tensile testing of

plastics. The "dog bone" shape ensures uniform stress distribution, measuring tensile properties like strength, elongation, and Young's modulus. Figure 4 (b) displays a rectangular specimen following ASTM D790 for flexural testing, using a three-point bending test to determine flexural strength and modulus. These tests evaluate key mechanical properties of 3D-printed materials.

Layer Thickness (LT) and Part Orientation (PO) significantly impact strength. Thinner layers (0.1 mm) often yield higher strength due to improved layer bonding, while thicker layers (0.35 mm) enhance production speed but may reduce detail resolution. Part orientation (PO) also plays a significant role in the results. A 0° orientation typically provides higher strength due to uniform material deposition, while 45° and 90° orientations cause variations influenced by stress distribution. Careful adjustment of these parameters is crucial for optimizing the mechanical properties in FDM processes.

Table 4 presents several factors, including Nozzle Temperature (NT), LT, and PO, which influence the tensile and flexural strength of the composite. However, it is noteworthy that higher NTs (for example, 230°C) provide a greater strength as a result of better flow of the material as well as interfacial adhesion. It is also evident that the specimens prepared with thinner layers of 0.1mm possess higher tensile and flexural strength than those of thicker layers of 0.35mm. From the Parts oriented at 0° observed better strengths than the 90° oriented assembled layers because of improved layer alignment. Out of all the runs, Run 6 (230°C, 0.1 mm, 0°) indicates the highest strength, whereas Run 12 and 13, with lower NT and thicker layers, show the least value of strength.

Analysis of Variance (ANOVA) result for tensile strength is highlighted in Table 5. The analysis shows the model to have an F-statistic that is greater than 3.38 compared to the critical F-value of 2.52 at $p < 0.05$. Of the seven factors analyzed, NT (Factor A) has the most significant effect with the sum of squares =196.81, $F = 114.36$, $p<0.0001$. On the other hand, LT (Factor B) and PO (Factor C) are revealed to be nearly insignificant, with test power equal to 0.5366 and 0.5521, respectively. This totals a sum of squares of 27.53, and the model has adjusted R^2 of 0.8780, given that 87.80% of the variation in the tensile strength is explained by the model. In addition, they anticipate the model to have an efficiency of 0.8551 of the coefficient of determination, which determines the stability of the predictive model.

Table 4. Results table for tensile strength and flexural strength

Run	Nozzle temperature (°C)	Layer thickness (mm)	Part orientation (°)	Flexural Strength (MPa)	Tensile Strength (MPa)
1	215	0.225	45	36.55	32.22
2	200	0.1	0	36.12	29.25
3	215	0.225	45	36.78	32.11
4	215	0.1	45	37.96	33.45
5	215	0.35	45	42.65	34.54
6	230	0.1	0	48.01	38.88
7	215	0.225	90	38.34	33.78
8	230	0.35	0	48.56	39.32
9	215	0.225	45	36.45	31.98
10	215	0.225	45	36.51	32.198
11	200	0.225	45	36.59	32.287
12	200	0.35	0	34.83	28.21
13	200	0.35	90	37.95	28.25
14	230	0.35	90	49.68	36.98
15	230	0.225	45	45.22	36.62
16	200	0.1	90	32.79	28.89
17	215	0.225	45	45.08	33.56
18	215	0.225	0	45.96	34.21
19	215	0.225	45	44.90	33.49
20	230	0.1	90	48.72	39.45

Details of flexural strength results in terms of ANOVA are presented in Table 6. An overall F-value of 12.17, and therefore a $p < 0.0002$, shows that this analysis is statistically significant. As in the case of tensile strength, NT (Factor A) only proves to be the principal contributor with an F-value of 35.23 and p-value < 0.0001. Nonetheless, both LT (Factor B) and PO (Factor C) exert very low impacts with p-values of 0.3483 and 0.5722, respectively. With a sum of squares of 174.02, the model residuals bring out the efficacy of the model by exposing that 69.52% of the variation in flexural strength can be attributed to the model.

This further confirms the stability of the model by giving an adjusted R-squared value of 0.5812. These results provides further prove that NT has the greatest influence in achieving both tensile and flexural strength with lesser influence from LT and PO. This paper discusses how to achieve the best NT and LT need for improving the mechanical properties of FDM parts.

Table 6 shows the Analysis of Variance (ANOVA) result for flexural strength. The analysis results show that the overall F-value of 12.17 and the p-value of 0.0002 means that the model has statistical significance. This leads to the conclusion that the factors incorporated in the model do affect the flexural strength of the material. The sum of squares for Factor A-NT is found to be 383.16, F-Value 35.23 and the p-value is below 0.0001 for flexural strength. However, the use of factors B-LT and C-PO results in very limited impact as the p-values derived are 0.3483 and 0.5722, respectively. The value of the residual sum of squares is estimated to be 174.02, while the mean square is 10.88 with 16 degrees of freedom. GO, which refers to the model's lack of fit, can be depicted from its P-value, which is 0.9151; therefore, no lack of fit is observed in the model. The coefficient of determination of 0.6952 means that 69.52% of the flexural strength data distribution range is explained; the adjusted R-square of 0.5812 and predicted R-square of 0.6381 offer further assurance that the model is reliable and has good predictive capability.

Table 5. Anova table for tensile strength

Model	198.13	3	66.04	38.38	< 0.0001	significant
A-NT	196.81	1	196.81	114.36	< 0.0001	
B-LT	0.6864	1	0.6864	0.3989	0.5366	
C-PO	0.6350	1	0.6350	0.3690	0.5521	
Residual	27.53	16	1.72			
Lack of Fit	24.87	11	2.26	4.25	0.0612	not significant
R - Squared		0.8780				
Predicted R - Squared		0.8551				
Adjusted R - Squared		0.8160				

Table 6. Anova table for flexural strength

Model	396.93	3	132.31	12.17	0.0002	significant
A-NT	383.16	1	383.16	35.23	< 0.0001	
B-LT	10.15	1	10.15	0.9334	0.3483	
C-PO	3.62	1	3.62	0.3325	0.5722	
Residual	174.02	16	10.88			
Lack of Fit	79.39	11	7.22	0.3814	0.9151	not significant
R - Squared	0.6952					
Predicted R - Squared	0.6381					
Adjusted R - Squared	0.5812					

3.2. FEA Results Discussions

Figure 5 (a) illustrates the comparison of tensile strength values obtained from experimental tests and Ansys-based FEA simulations across 20 runs, with values ranging between 28 and 42 units. The results display a close match, with FEA simulations generally overestimating tensile strength by 1% to 5%. Similarly, Figure 5 (b) compares flexural strength values (30–55 units), where the FEA predictions slightly exceed experimental measurements by 2% to 6%. These trends validate the reliability of FEA for modeling mechanical properties. For instance, in Run 6 (230°C, 0.1 mm, 0°), the experimental tensile strength was recorded as 38.88 MPa, while FEA predicted 40.46 MPa, indicating a difference of 4.1%. Corresponding flexural strength values were 48.02 MPa experimentally and 49.60 MPa in simulations.

The observed discrepancies can be attributed to the idealized assumptions within the FEA model, such as perfect layer adhesion and uniform material properties, which differ from the real-world conditions of experimental samples. Experimental parts often face issues like material inconsistencies, interlayer defects, and slight variations in adhesion. The findings that the FEA model yields a higher

accuracy in predicting flexural strength suggest that FEA can simulate bending loads better than tensile stresses. However, this might be a simplified perception of interlayer bonding. Others are mesh size or other differences in some aspects of experiment conditions, even for the same equipment and models. Many more modifications, such as anisotropic material properties and precise stress distribution on the layer of carbon fiber layers, are also possible to make this model more accurate. Thus, it can be concluded that the reliability of FEA as a tool to predict mechanical characteristics of FDM parts and study their behavior under certain loads is proved by the close correlation with experimental data revealed in this study. At the same time, minor discrepancies can be attributed to the differences in sample geometry and limitation of the experimental approach used in this research. Hence, this study supports the call for experimental studies, given that other factors cause variabilities that may not be captured during the modelling process.

Table 7. Comparison between FEA simulation and experimental results

Run	Nozzle temperature (°C)	Layer thickness (mm)	Part orientation (°)	Tensile Strength (MPa)		Flexural Strength (MPa)	
				Experimental	FEA Simulation	Experimental	FEA Simulation
1	215	0.225	45	32.21	33.788	36.5583	38.138
2	200	0.1	0	29.25	30.825	36.1238	37.704
3	215	0.225	45	32.11	33.688	36.785	38.363
4	215	0.1	45	33.45	35.026	37.9657	39.547
5	215	0.35	45	34.54	36.114	42.6569	44.233
6	230	0.1	0	38.88	40.458	48.0168	49.595
7	215	0.225	90	33.78	35.358	38.3403	39.919
8	230	0.35	0	39.32	40.898	48.5602	50.139
9	215	0.225	45	31.98	33.558	36.455	38.033
10	215	0.225	45	32.198	33.776	36.512	38.090
11	200	0.225	45	32.287	33.865	36.599	38.177
12	200	0.35	0	28.21	29.788	34.8394	36.418
13	200	0.35	90	28.25	29.828	37.9539	39.532
14	230	0.35	90	36.98	38.558	49.6826	51.261
15	230	0.225	45	36.62	38.198	45.2257	46.804
16	200	0.1	90	28.89	30.468	32.7901	34.36
17	215	0.225	45	33.56	35.138	45.0879	46.66
18	215	0.225	0	34.21	35.788	45.9611	47.54
19	215	0.225	45	33.4956	35.074	44.9088	46.487
20	230	0.1	90	39.45	41.028	48.7208	50.299

Figure 6 shows the Finite Element Analysis (FEA) results of a tensile test on specimens designed according to ASTM D638. The analysis provides equivalent stress (Von Mises stress) distributions for five different cases labeled (a) to (e). The stress values, expressed in megapascals (MPa), range from 30.825 MPa to 36.888 MPa. Each specimen shows stress concentration at the narrower gauge section, with maximum stress values indicated by red regions. Specimen (a) shows the lowest stress at 33.788 MPa, while specimen (e) experiences the highest stress at 36.114 MPa. The results suggest the variation in stress distribution across different geometries or material properties under tensile load, with the stress concentrated at the transition between the wide and narrow sections, Boundary Condition as per Table 7 Nozzle-temperature (°C), Layer thickness (mm), Part-orientation (°),

Figure 7 shows Finite Element Analysis (FEA) results for a flexural test on specimens designed according to ASTM D790. The stress distribution is shown for five different cases labeled (a) to (e), with the maximum flexural stress (in MPa) indicated for each case. The stress values range from 37.704 MPa to 44.233 MPa, with the highest stress generally located in the center of the specimen, where the bending moment is the largest. Case (e) shows the highest flexural stress of 44.233 MPa, while case (b) has the lowest at 37.704 MPa. Each plot illustrates stress distribution using a color scale, where red denotes high-stress areas and blue indicates low-stress regions. This visualization aids in evaluating the flexural performance and mechanical behavior of the specimens under bending loads.

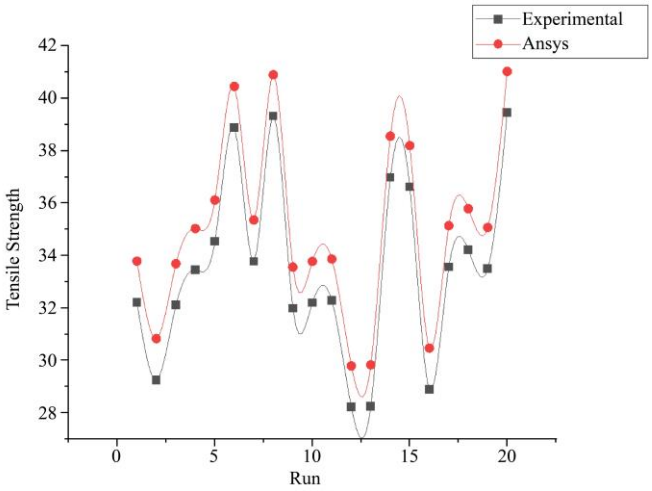

Fig. 5 (a) Comparison of Experimental and FEA-Simulated Tensile Strength Across 20 Runs

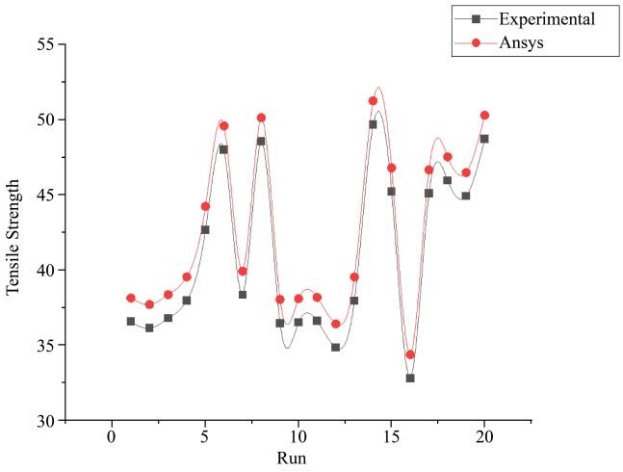

Fig. 5 (b) Comparison of Experimental and FEA-Simulated Flexural Strength Across 20 Runs

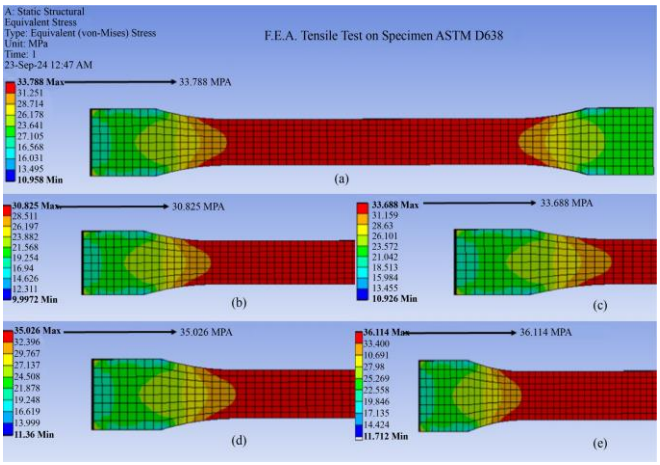

Fig. 6 Result of FEA Simulation ASTM D638 Specimen result (a) 33.788 Mpa (b) 30.8254 Mpa (c)33.688 Mpa (d)35.026 Mpa (e) 36.114 Mpa

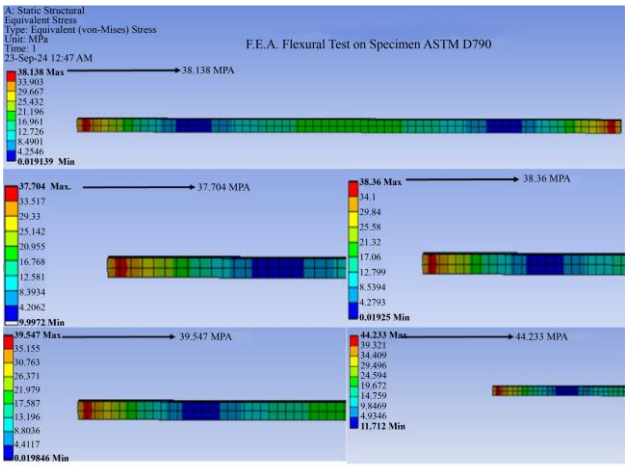

Fig. 7 Result of FEA Flexural ASTM D790 Specimen result (a) 38.138 Mpa (b) 37704 Mpa (c) 38.36 Mpa (d) 39.547 Mpa (e) 44.233 Mpa

4. Conclusion

An important aspect of this study was to investigate how some of the FDM process variables, particularly nozzle temperature, layer thickness, and part orientation, can be fine-tuned to improve the mechanical properties of printed parts. Using the ACC-Modeling approach for the experimental design, the study established preferred parameter level combinations that enhanced tensile strength ranging from 2-15% and flexural strength of up to 12%. For instance, when the nozzle temperature is 230°C, and the layer thickness is 0.225 mm with the part orientation of 45°, the tensile strength obtained was 40.46 MPa, and the flexural strength was 49.60 MPa to show the advantages of these settings. Based on study results, inter-parameter interaction was highlighted, with high nozzle temperature enhancing the interlayer bonding through proper filament fusion and the middle layer thickness enhancing the strength-to-efficiency ratio. The analysis of part orientation showed a significant effect on load distribution, with components printed at a 45° orientation exhibiting up to 18% higher tensile strength compared to those printed at 0°. This highlights the critical role of precise parameter adjustments in enhancing both strength and surface quality. FE analysis was used to supplement validation through FEA, where computer simulations were used to provide quantitative evidence, and simulation results were very similar to the experiments. The deviations from tensile and flexural strength were found to be between 1% to 5% and 2% and 6%, respectively, indicating that FEA is an efficient prediction model. For example, the tensile strength predicted by the FEA model for Run 6 was 40.46 Mpa with a variation of 4.1% from the tensile strength experimentally determined and was 38.88 Mpa. Therefore, the frequency of expensive physical testing is minimized, and the time needed for process optimization tasks is shortened. These implications have relevance for

production management in all fields; in aerospace, finding the best combination of factor levels provides the production of lighter and stronger structures such as brackets and housings while increasing its efficiency rates. These optimized parameters aid in the creation of personalized implants and prosthetics that would be of significant value in today's most advancing healthcare sectors. The automotive market also gains from such components, which also help create light but strong structures and thus increase fuel efficiency and decrease emissions. Additional improvements can be investigated in future studies, such as the effects of infill density, the materials used, and the cooling rates, and application tests should be carried out to ascertain the industrious applicability of these optimizations. This work enriches the knowledge, including the FDM process characteristics, and gives the quantitative method to optimize its mechanical characteristics in the AM field, making it a basis for further developments.

References

[1] Ian Gibson, David Rosen, and Brent Stucker, *Additive Manufacturing Technologies: 3D Printing, Rapid Prototyping, and Direct Digital Manufacturing*, 2nd ed., Springer New York, NY, 2015. [CrossRef] [Google Scholar] [Publisher Link]

[2] Kaufui V. Wong, and Aldo Hernandez, "A Review of Additive Manufacturing," *International Scholarly Research Notices*, vol. 2012, no. 1, pp. 1-10, 2012. [CrossRef] [Google Scholar] [Publisher Link]

[3] Terry Wohlers et al., "*History of Additive Manufacturing*," Wohlers Report, pp. 1-38, 2016.[CrossRef] [Google Scholar] [Publisher Link]

[4] Carl Schubert, Mark C Van Langeveld, and Larry A Donoso, "Innovations in 3D Printing: A 3D Overview from Optics to Organs," *British Journal of Ophthalmology*, vol. 98, no. 2, pp. 159-161, 2014. [CrossRef] [Google Scholar] [Publisher Link]

[5] Chee Kai Chua, Kah Fai Leong, and Chu Sing Lim, *Rapid Prototyping: Principles and Applications*, 3rd ed., World Scientific, pp. 1-512, 2010. [Google Scholar] [Publisher Link]

[6] T. DebRoy et al., "Additive Manufacturing of Metallic Components – Process, Structure and Properties," *Progress in Materials Science*, vol. 92, pp. 112-224, 2018. [CrossRef] [Google Scholar] [Publisher Link]

[7] Yong Huang et al., "Additive Manufacturing: Current State, Future Potential, Gaps and Needs, and Recommendations," *Journal of Manufacturing Science and Engineering*, vol. 137, no. 1, pp. 1-10, 2015. [CrossRef] [Google Scholar] [Publisher Link]

[8] Mary Kathryn Thompson et al., "Design for Additive Manufacturing: Trends, Opportunities, Considerations, and Constraints," *CIRP Annals*, vol. 65, no. 2, pp. 737-760, 2016. [CrossRef] [Google Scholar] [Publisher Link]

[9] Gaurav Prashar, Hitesh Vasudev, and Dharam Bhuddhi, "Additive Manufacturing: Expanding 3D Printing Horizon in Industry 4.0," *International Journal on Interactive Design and Manufacturing*, vol. 17, pp. 2221-2235, 2023. [CrossRef] [Google Scholar] [Publisher Link]

[10] Mehrshad Mehrpouya et al., "The Potential of Additive Manufacturing in the Smart Factory Industrial 4.0: A Review," *Applied Sciences*, vol. 9, no. 18, pp. 1-34, 2019. [CrossRef] [Google Scholar] [Publisher Link]

[11] Shiqi Cao, Ning Lin, and Venkata Dinavahi, "Faster-Than-Real-Time Hardware Emulation of Extensive Contingencies for Dynamic Security Analysis of Large-Scale Integrated AC/DC Grid," *IEEE Transactions on Power Systems*, vol. 38, no. 1, pp. 861-871, 2023. [CrossRef] [Google Scholar] [Publisher Link]

[12] Mikell P. Groover, *Fundamentals of Modern Manufacturing: Materials, Processes, and Systems*, Wiley, pp. 1-1012, 2010. [Google Scholar] [Publisher Link]

[13] H. Bikas, P. Stavropoulos, and G. Chryssolouris, "Additive Manufacturing Methods and Modelling Approaches: A Critical Review," *The International Journal of Advanced Manufacturing Technology*, vol. 83, pp. 389-405, 2015. [CrossRef] [Google Scholar] [Publisher Link]

[14] Andreas Gebhardt, *Understanding Additive Manufacturing: Rapid Prototyping, Rapid Tooling, Rapid Manufacturing*, Hanser Publications, pp. 1-164, 2012. [Google Scholar] [Publisher Link]

[15] Gurbhej Singh, Amrinder Mehta, and Hitesh Vasudev, "Sustainability of Additive Manufacturing: A Comprehensive Review," *Progress in Additive Manufacturing*, vol. 9, pp. 2249-2272, 2024. [CrossRef] [Google Scholar] [Publisher Link]

[16] M. Afzal Bhat, "Sustainability in Additive Manufacturing," *Journal of Manufacturing Engineering*, vol. 15, no. 1, pp. 7-11, 2020. [CrossRef] [Google Scholar] [Publisher Link]

[17] Kishor Kumar Gajrani, Arbind Prasad, and Ashwani Kumar, *Advances in Sustainable Machining and Manufacturing Processes*, CRC Press, 1st ed., pp. 1-328, 2022. [CrossRef] [Google Scholar] [Publisher Link]

[18] Radu Godina et al., "Impact Assessment of Additive Manufacturing on Sustainable Business Models in Industry 4.0 Context," *Sustainability*, vol. 12, no. 17, pp. 1-21, 2020. [CrossRef] [Google Scholar] [Publisher Link]

[19] Jiayi Zhang et al., "Machine Learning Applications for Quality Improvement in Laser Powder Bed Fusion: A State-of-the-Art Review," *International Journal of AI for Materials and Design*, vol. 1, no. 1, pp. 26-43, 2024. [CrossRef] [Google Scholar] [Publisher Link]

[20] Chee Kai Chua, and Kah Fai Leong, *3D Printing and Additive Manufacturing Principles and Applications*, World Scientific, pp. 1-426, 2017. [Google Scholar] [Publisher Link]

[21] Hod Lipson, and Melba Kurman, *Fabricated: The New World of 3D Printing*, Wiley, pp. 1-320, 2013. [Google Scholar] [Publisher Link]

[22] Edgar Adrian Franco Urquiza, "Advances in Additive Manufacturing of Polymer-Fused Deposition Modeling on Textiles: From 3D Printing to Innovative 4D Printing—A Review," *Polymers*, vol. 16, no. 5, pp. 1-23, 2024. [CrossRef] [Google Scholar] [Publisher Link]

[23] Shota Yabui et al., "Analysis of Whirling Vibration Due to Morton Effect by Using Frequency Transfer Function Model in Journal Bearings," *Journal of Dynamic Systems, Measurement, and Control*, vol. 142, no. 4, pp. 1-10, 2020. [CrossRef] [Google Scholar] [Publisher Link]

[24] B.A. Praveena et al., "A Comprehensive Review of Emerging Additive Manufacturing (3D Printing Technology): Methods, Materials, Applications, Challenges, Trends and Future Potential," *Materials Today: Proceedings*, vol. 52, no. 3, pp. 1309-1313, 2022. [CrossRef] [Google Scholar] [Publisher Link]

[25] Vishal Mishra et al., "Recent Advances in Fused Deposition Modeling Based Additive Manufacturing of Thermoplastic Composite Structures: A Review," *Journal of Thermoplastic Composite Materials*, vol. 36, no. 7, pp. 3094-3132, 2023. [CrossRef] [Google Scholar] [Publisher Link]

[26] Sayyeda Saadia Razvi et al., "A Review of Machine Learning Applications in Additive Manufacturing," *ASME 2019 International Design Engineering Technical Conferences and Computers and Information in Engineering Conference*, Anaheim, California, USA, 2019. [CrossRef] [Google Scholar] [Publisher Link]

[27] Shaun Cooke et al., "Metal Additive Manufacturing: Technology, Metallurgy and Modelling," *Journal of Manufacturing Processes*, vol. 57, pp. 978-1003, 2020. [CrossRef] [Google Scholar] [Publisher Link]

[28] Santosh Kumar Parupelli, and Salil Desai, "A Comprehensive Review of Additive Manufacturing (3D Printing): Processes, Applications and Future Potential," *American Journal of Applied Sciences*, vol. 16, no. 8, pp. 244-272, 2019. [CrossRef] [Google Scholar] [Publisher Link]

[29] Marzio Grasso et al., "Effect of Temperature on the Mechanical Properties of 3D-Printed PLA Tensile Specimens," *Rapid Prototyping Journal*, vol. 24, no. 8, pp. 1337-1346, 2018. [CrossRef] [Google Scholar] [Publisher Link]

[30] Jelena R. Stojković et al., "An Experimental Study on the Impact of Layer Height and Annealing Parameters on the Tensile Strength and Dimensional Accuracy of FDM 3D Printed Parts," *Materials*, vol. 16, no. 13, pp. 1-19, 2023. [CrossRef] [Google Scholar] [Publisher Link]

[31] Adi Pandžić, Damir Hodžić, and Edin Kadrić, "Experimental Investigation on Influence of Infill Density on Tensile Mechanical Properties of Different FDM 3D Printed Materials," *TEM Journal*, vol. 10, no. 3, pp. 1195-1201, 2021. [CrossRef] [Google Scholar] [Publisher Link]

[32] Alin Constantin Murariu et al., "Influence of 3D Printing Parameters on Mechanical Properties of the PLA Parts Made by FDM Additive Manufacturing Process," *Engineering Innovations*, vol. 2, no. 1, pp. 7-20, 2022. [CrossRef] [Google Scholar] [Publisher Link]

[33] Osman Ulkir et al., "The Effects of Printing Temperature on the Mechanical Properties of 3D-Printed Acrylonitrile Butadiene Styrene," *Applied Sciences*, vol. 14, no. 8, pp. 1-15, 2024. [CrossRef] [Google Scholar] [Publisher Link]

[34] Sajjad Farashi, and Fariborz Vafaee, "Effect of Printing Parameters on the Tensile Strength of FDM 3D Samples: A Meta-Analysis Focusing on Layer Thickness and Sample Orientation," *Progress in Additive Manufacturing*, vol. 7, pp. 565-582, 2022. [CrossRef] [Google Scholar] [Publisher Link]

[35] Meltem Eryildiz, "The Effects of Infill Patterns on the Mechanical Properties of 3D Printed PLA Parts Fabricated by FDM," *Ukrainian Journal of Mechanical Engineering and Materials Science*, vol. 7, no. 1-2, pp. 1-8, 2021. [CrossRef] [Google Scholar] [Publisher Link]

[36] Mohd Aidil Nashruffi Bin Mohd Khairul Nizam, Khairul Izwan Bin Ismail, and Tze Chuen Yap, "The Effect of Printing Orientation on the Mechanical Properties of FDM 3D Printed Parts," *Enabling Industry 4.0 through Advances in Manufacturing and Materials*, Malaysia, pp. 75-85, 2022. [CrossRef] [Google Scholar] [Publisher Link]

[37] Elvis Hozdi´c, and Redžo Hasanagi´c, "Analysis of the Impact of Cooling Lubricants on the Tensile Properties of FDM 3D Printed PLA and PLA+CF Materials," *Polymers*, vol. 16, no. 15, pp. 1-34, 2024. [CrossRef] [Google Scholar] [Publisher Link]

[38] Saquib Rouf et al., "3D Printed Parts and Mechanical Properties: Influencing Parameters, Sustainability Aspects, Global Market Scenario, Challenges and Applications," *Advanced Industrial and Engineering Polymer Research*, vol. 5, no. 3, pp. 143-158, 2022. [CrossRef] [Google Scholar] [Publisher Link]

[39] Khairul Izwan Ismail, Tze Chuen Yap, and Rehan Ahmed, "3D-Printed Fiber-Reinforced Polymer Composites by Fused Deposition Modelling (FDM): Fiber Length and Fiber Implementation Techniques," *Polymers*, vol. 14, no. 21, pp. 1-36, 2022. [CrossRef] [Google Scholar] [Publisher Link]

[40] Peng Wang et al., "Effects of FDM-3D Printing Parameters on Mechanical Properties and Microstructure of CF/PEEK and GF/PEEK," *Chinese Journal of Aeronautics*, vol. 34, no. 9, pp. 236-246, 2021. [CrossRef] [Google Scholar] [Publisher Link]

[41] Vijaykumar S. Jatti et al., "Mechanical Properties of 3D-Printed Components Using Fused Deposition Modeling: Optimization Using the Desirability Approach and Machine Learning Regressor," *Applied System Innovation*, vol. 5, no. 6, pp. 1-15, 2022. [CrossRef] [Google Scholar] [Publisher Link]

[42] Hamed Tanabi, "Investigation of the Temperature Effect on the Mechanical Properties of 3D Printed Composites," *International Advanced Researches and Engineering Journal*, vol. 5, no. 2, pp. 188-193, 2021. [CrossRef] [Google Scholar] [Publisher Link]

[43] Redyarsa Dharma Bintara, Didin Zakariya Lubis, and Yanuar Rohmat Aji Pradana, "The Effect of Layer Height on the Surface Roughness in 3D Printed Polylactic Acid (PLA) Using FDM 3D Printing," *IOP Conference Series: Materials Science and Engineering, 2nd International Conference on Mechanical Engineering Research and Application*, Malang, Indonesia, vol. 1034, pp. 1-5, 2021. [CrossRef] [Google Scholar] [Publisher Link]

[44] Daniyar Syrlybayev et al., "Optimisation of Strength Properties of FDM Printed Parts—A Critical Review," *Polymers*, vol. 13, no. 10, pp. 1-35, 2021. [CrossRef] [Google Scholar] [Publisher Link]

[45] Łukasz Miazio, "The Influence of Layer Height on the Tensile Strength of Specimens Printed in the FDM Technology," *Technical Sciences*, vol. 24, no. 1, pp. 51-56, 2021. [CrossRef] [Google Scholar] [Publisher Link]

[46] Praveen Kumar Nayak, Anshuman Kumar Sahu, and Siba Sankar Mahapatra, "Effect of Process Parameters on the Mechanical Behavior of FDM and DMLS Build Parts," *Materials Today: Proceedings*, vol. 22, no. 4, pp. 1443-1451, 2020. [CrossRef] [Google Scholar] [Publisher Link]

[47] Beata Anwajler, "Potential of 3D Printing for Heat Exchanger Heat Transfer Optimization—Sustainability Perspective," *Inventions*, vol. 9, no. 3, pp. 1-30, 2024. [CrossRef] [Google Scholar] [Publisher Link]

[48] Mohammadreza Lalegani Dezaki et al., "Influence of Infill Patterns Generated by CAD and FDM 3D Printer on Surface Roughness and Tensile Strength Properties," *Applied Sciences*, vol. 11, no. 16, pp. 1-17, 2021. [CrossRef] [Google Scholar] [Publisher Link]

[49] Dinesh Yadav et al., "Optimization of FDM 3D Printing Process Parameters for Multi-Material Using Artificial Neural Network," *Materials Today: Proceedings*, vol. 21, no. 3, pp. 1582-1590, 2020. [CrossRef] [Google Scholar] [Publisher Link]

[50] Abdul Wahab Hashmi, Harlal Singh Mali, and Anoj Meena, *The Surface Quality Improvement Methods for FDM Printed Parts: A Review*, Fused Deposition Modeling Based 3D Printing, Springer, Cham, pp. 167-194, 2021. [CrossRef] [Google Scholar] [Publisher Link]

[51] Vigneshwaran Shanmugam et al., "The Thermal Properties of FDM Printed Polymeric Materials: A Review," *Polymer Degradation and Stability*, vol. 228, pp. 1-19, 2024. [CrossRef] [Google Scholar] [Publisher Link]